

# COMPARISON BETWEEN SINGLE PARTICLE ENERGY STATES OF $\Lambda$ -HYPERNUCLEUS AND $\Sigma^-$ -HYPERNUCLEUS WITH WOODS-SAXON POTENTIAL

Thida Wint<sup>1</sup>, Win Win Maw<sup>2</sup>, Maung Maung Chit<sup>3</sup> and Khin Swe Myint<sup>4</sup>

## Abstract

In this research,  $\Lambda$  and  $\Sigma^-$  single particle energy states are compared to study the role of  $\Lambda$  and  $\Sigma^-$  hyperons in nuclear medium. Energy states are calculated by solving one body Schrödinger equation with Woods-Saxon central potential including central part and spin-orbit coupling. Coulomb potential is taken into account for the calculation of  $\Sigma^-$  particle energy states. Wave function expanded into Gaussian basis is used in our calculation. Root-mean-square distance for various orbital angular momentum states are also calculated. The characteristic of  $\Lambda$  and  $\Sigma^-$  single particle energy states in light and heavy nuclei are discussed.

**Keywords:**  $\Lambda$  single particle energy states,  $\Sigma^-$  single particle energy states, Woods-Saxon potential, Coulomb potential

## Introduction

For the study of nuclear physics, the baryon-baryon interaction is fundamental and important. To complete the knowledge of baryon-baryon interaction, it is essential to understand Nucleon (N)-Nucleon (N) interaction, Hyperon (Y)-Nucleon (N) interaction, Y-Y interaction which can be obtained from normal nuclei, strangeness -1 ( $S = -1$ ) hypernuclei and strangeness -2 ( $S = -2$ ) hypernuclei respectively. N-N interaction has been continuously studied for more than 60 years. Regarding the Y-N interaction and Y-Y interaction, where Y is a  $\Sigma$  or  $\Lambda$  hyperon, its research is steadily progressing. For strangeness ( $S = -1$ ) system, about 40  $\Lambda$ -hypernuclei and one  $\Sigma^-$ -hypernucleus were found experimentally [Bando H, Motoba T and Zofka J, 1990]. Hyperons do not suffer from Pauli blocking by the other nucleons, it can penetrate into the nuclear interior and form deeply bound hypernuclear states. However, it is predicted that the average  $\Sigma$  potential in nuclear matter must be shallow due to the  $\Sigma \rightarrow \Lambda$  strong conversion channel. There are many open questions about  $\Sigma^-$  hypernuclei such as production reaction, widths and related Coulomb field assistance, quasi-free spectrum competition and decay channels. It is difficult to get the information about the  $\Sigma^-$ -hypernuclear states from experimental data with low statistics. Due to lack of the information on a phenomenological side, the theoretical calculation plays an important role in understanding the behavior of a  $\Sigma^-$ -hyperon in nuclei.

In this research, single particle energy states of  $\Lambda$ -hyperon and  $\Sigma^-$ -hyperon in light hypernuclei  ${}_{\Lambda}^{16}O$  and  ${}_{\Sigma^-}^{16}C$  and heavy hypernuclei  ${}_{\Lambda}^{208}Pb$  and  ${}_{\Sigma^-}^{208}Hg$  are investigated to study the role of  $\Lambda$  and  $\Sigma^-$  hyperons in nuclear medium. In this calculation, we considered that a  $\Lambda$  or  $\Sigma^-$  hyperon moves freely in an average potential well generated by the other nucleons. Energy states are calculated by solving one body Schrödinger equation with Woods-Saxon central potential including spin-orbit coupling. Coulomb potential is taken into account for the calculation of  $\Sigma^-$  particle states to investigate the Coulomb effect in  $\Sigma^-$ -hypernuclei. Gaussian basis wave is used as a trial wave function in our calculation. Root-mean-square (RMS) distance for various orbital angular momentum states are also calculated.  $\Lambda$  and  $\Sigma^-$  single particle energy states in light and

heavy nuclei are calculated and discussed about the characteristic of those two hyperons in different nuclear medium.

### Solving the Schrödinger Equation with the Gaussian Basis Wave Function

Single particle energy levels of a hyperon in a potential well are numerically determined by solving the Schrödinger radial equation using the power inverse iteration method.

The Schrödinger Radial Equation (SRE) is

$$\frac{d^2u(r)}{dr^2} + \frac{2m}{\hbar^2} \left[ E - V(r) - \frac{\hbar^2}{2m} \frac{l(l+1)}{r^2} \right] u(r) = 0 \quad (1)$$

where  $u(r) = rR_{nl}$  is the reduced radial wave function.

$$u(r) = r^{\ell+1} \sum_{j=1}^N c_j e^{-\left(\frac{r}{b_j}\right)^2} \quad (2)$$

where  $b_j$ 's are the range parameter and are chosen to be geometric progression as follows.

$\frac{b_2}{b_1} = \frac{b_3}{b_2} = \frac{b_4}{b_3} = \dots = \text{constant}$ ,  $b_{i+1} = \left(\frac{b_N}{b_1}\right)^{1/N-1} b_i$  and  $N$  is the number of coefficients and,  $c_j$ 's are expansion coefficients.

The Schrödinger equation is written as follow.

$$(H_0 + V) u = E u$$

where,  $E$  = energy eigen value,  $u$  = eigen vector,  $H_0$  = kinetic energy operator and  $V$  = potential energy operator.

The Schrödinger equation for radial part is,

$$\left\{ -\frac{\hbar^2}{2M} \frac{d^2}{dr^2} + \frac{\hbar^2}{2M} \frac{l(l+1)}{r^2} + V(r) \right\} u(r) = E u(r) \quad (3)$$

$$\left\{ -\frac{\hbar^2}{2M} \frac{d^2}{dr^2} + \frac{\hbar^2}{2M} \frac{l(l+1)}{r^2} + V(r) \right\} r^{\ell+1} \sum_{j=1}^N c_j e^{-\left(\frac{r}{b_j}\right)^2} = E r^{\ell+1} \sum_{j=1}^N c_j e^{-\left(\frac{r}{b_j}\right)^2} \quad (4)$$

Multiplying both sides of the equation by  $r^{\ell+1} e^{-\left(\frac{r}{b_i}\right)^2}$  from the left and integration through the equation

$$\int r^{\ell+1} e^{-\left(\frac{r}{b_i}\right)^2} \left\{ -\frac{\hbar^2}{2M} \frac{d^2}{dr^2} + \frac{\hbar^2}{2M} \frac{l(l+1)}{r^2} + V(r) \right\} \sum_j c_j r^{\ell+1} e^{-\left(\frac{r}{b_j}\right)^2} dr = E \int r^{\ell+1} e^{-\left(\frac{r}{b_i}\right)^2} \sum_j c_j r^{\ell+1} e^{-\left(\frac{r}{b_j}\right)^2} dr \quad (5)$$

We can define the above equation as

$$\sum_j [T_{ij} + V_{\ell ij} + V_{ij}] c_j = E \sum_j N_{ij} c_j \tag{6}$$

where  $T_{ij}$  is kinetic energy matrix element,  $N_{ij}$  is norm matrix element and  $V_{\ell ij}$  is the centrifugal potential energy matrix element.  $H_{ij}$  is Hamiltonian matrix element. The  $N_{ij}$ ,  $T_{ij}$  and  $V_{\ell ij}$  are analytically solved by using standard integral form as follows.

The norm matrix element, 
$$N_{ij} = \int r^{\ell+1} e^{-\left(\frac{r}{b_i}\right)^2} r^{\ell+1} e^{-\left(\frac{r}{b_j}\right)^2} dr$$

The kinetic energy matrix element, 
$$T_{ij} = \int r^{\ell+1} e^{-\left(\frac{r}{b_i}\right)^2} \left\{ -\frac{\hbar^2}{2\mu} \frac{d^2}{dr^2} \right\} r^{\ell+1} e^{-\left(\frac{r}{b_j}\right)^2} dr$$

The centrifugal potential energy matrix element, 
$$V_{\ell ij} = \int r^{\ell+1} e^{-\left(\frac{r}{b_i}\right)^2} \frac{\ell(\ell+1)}{r^2} r^{\ell+1} e^{-\left(\frac{r}{b_j}\right)^2} dr$$

The potential energy matrix element, 
$$V_{ij} = \int r^{\ell+1} e^{-\left(\frac{r}{b_i}\right)^2} V r^{\ell+1} e^{-\left(\frac{r}{b_j}\right)^2} dr$$
 The Hamiltonian matrix

element, 
$$H_{ij} = \int r^{\ell+1} e^{-\left(\frac{r}{b_i}\right)^2} H r^{\ell+1} e^{-\left(\frac{r}{b_j}\right)^2} dr$$

where 
$$H_{ij} = T_{ij} + V_{\ell ij} + V_{ij}.$$

The Schrödinger equation in matrix form can be written as follows.

$$[H] [C] = E [N] [C] \tag{7}$$

Equation (7) can be expanded as

$$\begin{aligned} H_{11} C_1 + H_{12} C_2 + \dots + H_{1N} C_N &= E (N_{11} C_1 + N_{12} C_2 + \dots + N_{1N} C_N) \\ H_{21} C_1 + H_{22} C_2 + \dots + H_{2N} C_N &= E (N_{21} C_1 + N_{22} C_2 + \dots + N_{2N} C_N) \\ H_{N1} C_1 + H_{N2} C_2 + \dots + H_{NN} C_N &= E (N_{N1} C_1 + N_{N2} C_2 + \dots + N_{NN} C_N), \end{aligned}$$

which are

$$\sum_{i,j=0}^N (H_{ij} - E N_{ij}) C_j = 0$$

In order to determine the energy eigen value E, we solved the following set of linear equations iteratively.

$$\sum_{i,j=0}^N (H_{ij} - E_0 N_{ij}) C_j^{(k)} = \sum_{i,j=0}^N N_{ij} C_j^{(k-1)}, k = 1, 2, \dots, \ell \tag{8}$$

With 
$$E = E_0 + \frac{C_j^{(k-1)}}{C_j^{(k)}}$$

where  $E_0$  =initial guess value of energy

$E$  = energy eigen value,  $N$  = number of coefficients,  $C$  = expansion coefficient, and  $\ell$  = number of iterations.

The convergence of iteration is obtained when the ratio of  $\frac{C_j^{(k-1)}}{C_j^{(k)}}$  becomes constant. i.e.,

$$\frac{C_j^{(k-2)}}{C_j^{(k-1)}} = \frac{C_j^{(k-1)}}{C_j^{(k)}}$$

### Average Potential Well of a $\Lambda$ -Hypernucleus

The interaction between lambda and the other nucleons in the core nucleus is derived using phenomenological Woods-Saxon potential which is based upon the sum of a spin-independent central potential and spin-orbit potential. In our calculation, we considered that a  $\Lambda$ -particle moves freely in an average potential well generated by the other nucleons of the core nucleus. The total nuclear interaction between lambda and core nucleus is

$$V(r) = V_l(r) + V_{w-s}(r) + V_{l-s}(r) \quad (9)$$

where,  $V_l(r)$  = centrifugal potential = 
$$\frac{\hbar^2}{2m_\Lambda} \frac{\ell(\ell+1)}{r^2}$$

$m_\Lambda$  =the mass of lambda and  $l$  =orbital angular momentum quantum number.

$$V_{l-s}(r) = \text{Woods-Saxon spin-orbit potential} = V_{so} \left( \frac{\hbar}{m_\pi c} \right)^2 \left( \frac{\vec{\ell} \cdot \vec{s}}{\ell} \right) \frac{1}{r} \frac{d\rho}{dr}$$

If total angular momentum  $j = \ell + \frac{1}{2}$ ,  $V_{l-s}(r) = V_{so} \left( \frac{\hbar}{m_\pi c} \right)^2 \left( \frac{1}{2} \ell \right) \frac{1}{r} \frac{d\rho}{dr}$

If total angular momentum  $j = \ell - \frac{1}{2}$ ,  $V_{l-s}(r) = V_{so} \left( \frac{\hbar}{m_\pi c} \right)^2 \left[ -\frac{1}{2}(\ell+1) \right] \frac{1}{r} \frac{d\rho}{dr}$

$V_{so}$  = the strength of Woods-Saxon spin-orbit coupling potential term

$$\frac{\hbar}{m_\pi c} = \text{Compton wavelength of the pion}$$

$$V_{w-s}(r) = \text{Woods-Saxon central potential} = -V_0 \rho(r)$$

$V_0$  = the strength of the Woods-Saxon potential

$$\rho(r) = \text{the nuclear density} = \frac{1}{\frac{r-R}{1 + e^{-a}}}$$

In above equation,  $r$  = the radial distance from the center,

$$R = \text{the nuclear radius} \left( R = r_0 (A - 1)^{\frac{1}{3}} \right)$$

$a$  = the diffuseness parameter.

The total interaction between lambda and core nucleus becomes

$$V(r) = \frac{\hbar^2}{2m_\Lambda} \frac{\ell(\ell+1)}{r^2} - \frac{V_0}{1 + e^{-r/R/a}} - V_{SO} \left( \frac{\hbar}{m_\pi c} \right)^2 \left( \frac{\ell}{2} \right) \frac{1}{ra} \frac{e^{-r/R/a}}{\left( 1 + e^{-r/R/a} \right)^2} \quad \text{for } j = \ell + \frac{1}{2} \quad 10(a)$$

$$V(r) = \frac{\hbar^2}{2m_\Lambda} \frac{\ell(\ell+1)}{r^2} - \frac{V_0}{1 + e^{-r/R/a}} + V_{SO} \left( \frac{\hbar}{m_\pi c} \right)^2 \left( \frac{1}{2}(\ell+1) \right) \frac{1}{ra} \frac{e^{-r/R/a}}{\left( 1 + e^{-r/R/a} \right)^2} \quad \text{for } j = \ell - \frac{1}{2} \quad (b)$$

Using above potentials as in 10(a) and (b),  $\Lambda$ -single particle energy states in  $^{16}_\Lambda O$  and  $^{208}_\Lambda Pb$  are calculated for different  $lj$  states.

### Average Potential Well of a $\Sigma^-$ -Hypernucleus

In contrast to  $\Lambda$ -hypernuclei where the narrow peak in experimental excitation spectra indicate correctness of the notion of a single particle, such a property for the  $\Sigma$ -hyperon is not so well established. The observation of the ground state of as light species as  $\Sigma^-$ -hyperhelium  $^4_\Sigma He$  was announced at the 1988 Padova Conference [Hayano R S *et al.*, 1988]. The ( $K^-$  stopped,  $\pi^-$ ) reaction produced ground state at as much as  $3.2 \pm 0.3$  MeV binding with a width of  $4.6 \pm 0.5$  MeV [Harada T and Akaishi Y, 1990][Bressani T *et al.*, 1989]. Such a  $\Sigma$ -hypernucleus state was derived also theoretically with full use of the repulsive core and strong isospin-spin dependence of the  $\Sigma$ -N interaction. In the reference [Hayano R S *et al.*, 1988], the authors claimed that the width may reach as much as a few tens of MeV in nuclear matter due to  $\Sigma \rightarrow \Lambda$  strong conversion channel and the average  $\Sigma$ -nucleus potential must be shallow (well depth of  $10 \leq V_{re} \leq 25$  MeV). The spin-orbit splitting seems to be comparable (or larger) than that for a nucleon. For a long time, the strength of the  $\Sigma$  spin-orbit potential ( $V_{so}$ ) was intensively discussed [Dover C B, 1986]. It was usually believed that its amount may distinguish between quark-gluon and meson-exchange pictures of baryon-nucleon interactions. In a simple additive quark model [Pirner H J, 1979] [Pirner H J and Povh B, 1982] a large  $\Sigma$  spin-orbit potential was predicted:

$$V_{so}^N : V_{so}^\Lambda : V_{so}^\Sigma : V_{so}^\Xi = 1 : 0 : \frac{4}{3} : -\frac{1}{3},$$

Where as OBE models [Bando H, 1981] predict much smaller values ( $V_{so}^\Sigma \sim V_{so}^N / 3$ ,  $V_{so}^\Xi \sim V_{so}^\Lambda$ ). The experiments [Bertini *et al.*, 1985][Yamazaki T *et al.*, 1986] in the mid-eighties supported the

idea of large  $\Sigma$  spin-orbit strength and thus the quark model. Large  $\Sigma$  spin-orbit strength [Dover C B, 1986] would contradict both quark and OBE models. New data are needed to settle this problem.

In this research,  $\Sigma$  spin-orbit strength ( $V_{so}$ ) is used as 18 MeV according to the reference [Wünsch R and Zofka J, 1988]. Attractive Coulomb interaction is also taken into account for the interaction between  $\Sigma^-$  and core nucleus. The total interaction between  $\Sigma^-$  and core nucleus is

$$V(r) = V_l(r) + V_{w-s}(r) + V_{is}(r) + V_c(r)$$

$V_c$  is the Coulomb potential of a homogeneously charged sphere with the radius  $R_c$ . The value  $R_c = 1.25 (A-1)^{1/3}$  fm, is used in this calculation.

The total interaction between  $\Sigma^-$  and the other nucleons in core nucleus for  $j = l+1/2$  and for  $j = l-1/2$  are as in following equations 11(a) and (b).

$$V(r) = \frac{\hbar^2}{2m_\Sigma} \frac{\ell(\ell+1)}{r^2} - \frac{V_0}{1+e^{-r-R/a}} - V_{so} \left( \frac{\hbar}{m_\pi c} \right)^2 \left( \frac{1}{2} \ell \right) \frac{1}{ra} \frac{e^{-r-R/a}}{\left( 1+e^{-r-R/a} \right)^2} + V_c(r) \quad 11(a)$$

$$V(r) = \frac{\hbar^2}{2m_\Sigma} \frac{\ell(\ell+1)}{r^2} - \frac{V_0}{1+e^{-r-R/a}} + V_{so} \left( \frac{\hbar}{m_\pi c} \right)^2 \left( \frac{1}{2} (\ell+1) \right) \frac{1}{ra} \frac{e^{-r-R/a}}{\left( 1+e^{-r-R/a} \right)^2} + V_c(r) \quad 11(b)$$

Due to  $\Sigma \rightarrow \Lambda$  strong conversion channel, the complex potential is used in which real part of potential gives the bonding energy and imaginary part gives the level width of  $\Sigma^-$  single particle states in  $\Sigma$ -hypernuclei. The parameters which are used in this calculation are summarized in table (1).

**Table 1 The potential and range parameters used in our calculation [Bando H *et al.*, 1990]**

Types of Parameter	$\Lambda$ hypernuclei	$\Sigma^-$ hypernuclei
strength of Woods-Saxon central potential	-30 MeV	(-10 - i3) MeV
Diffuseness parameter (a)	0.6 fm	0.6 fm
Radius of single nucleon ( $r_0$ )	1.1 fm	1.1 fm
Strength of spin-orbit potential	-4 MeV	-18 MeV

## Results and Discussions

In order to know the attractive Coulomb interaction effect in  $\Sigma^-$ -hypernuclei, the energy eigen values of  $\Sigma^-$ hypernuclei are calculated within the frame work of Woods-Saxon central potential with and without Coulomb interaction. The results are compared in figure (1).

To investigate the role of  $\Lambda$  and  $\Sigma$  hyperons in hypernuclei, single particle states and root mean square distance of light hypernuclei  ${}^{16}_{\Lambda}O$  and  ${}^{16}_{\Sigma^{-}}C$  and heavy hypernuclei  ${}^{208}_{\Lambda}Pb$  and  ${}^{208}_{\Sigma^{-}}Hg$  are calculated and the results are compared in table (2) to (5). Energy states are also displayed in figure (2) and (3).

**Table 2  $\Lambda$  and  $\Sigma$  single particle states of light hypernuclei  ${}^{16}_{\Lambda}O$  and  ${}^{16}_{\Sigma^{-}}C$  for different  $lj$  states**

Single-particle States	${}^{16}_{\Lambda}O$	${}^{16}_{\Sigma^{-}}C$		Single particle states	${}^{16}_{\Lambda}O$	${}^{16}_{\Sigma^{-}}C$	
	Single particle energy (MeV)	Single particle energy (MeV) (without Coulomb Potential)	Single particle energy (MeV) (with Coulomb Potential)		Single particle energy (MeV)	Single particle energy (MeV) (without Coulomb potential)	Single particle energy (MeV) (with Coulomb potential)
1s	-13.04	-1.07-1.27	-4.79-1.60	$1s_{1/2}$	-13.04	-1.07-1.27	-4.79-1.60
1p	-2.34	-	-0.21-0.24	$1p_{3/2}$	-2.76	-	-2.01-0.89
				$1p_{1/2}$	-1.54	-	-

**Table 3 Root-mean-square distance of light hypernuclei  ${}^{16}_{\Lambda}O$  and  ${}^{16}_{\Sigma^{-}}C$  for different  $lj$  states**

Single-particle States	RMS distance (fm)	RMS distance (fm) (without Coulomb potential)	RMS distance (fm) (with Coulomb potential)	Single-particle States	RMS distance (fm)	RMS distance (fm) (without Coulomb potential)	RMS distance (fm) (with Coulomb potential)
1s	2.19	3.87	3.03	$1s_{1/2}$	2.19	3.87	3.03
1p	3.34	-	8.34	$1p_{3/2}$	3.28	-	4.27
				$1p_{1/2}$	3.48	-	-

**Table 4**  $\Lambda$  and  $\Sigma$  single particle states of heavyhypernuclei  ${}^{208}_{\Lambda}Pb$  and  ${}^{208}_{\Sigma^{-}}Hg$  for different  $lj$ states

Single-particle States	${}^{208}_{\Lambda}Pb$	${}^{208}_{\Sigma^{-}}Hg$		Single particle states	${}^{208}_{\Lambda}Pb$	${}^{208}_{\Sigma^{-}}Hg$	
	Single particle energy (MeV)	Single particle energy (MeV) (without Coulomb Potential)	Single particle energy (MeV) (with Coulomb Potential)		Single particle energy (MeV)	Single particle energy (MeV) (without Coulomb potential)	Single particle energy (MeV) (with Coulomb potential)
1s	-25.86	-6.99-2.76	-30.99-2.92	$1s_{1/2}$	-25.86	-6.99-2.76	-30.99-2.92
1p	-21.85	-4.16-2.48	-26.69-2.80	$1p_{3/2}$	-21.91	-5.03-2.39	-27.22-2.75
				$1p_{1/2}$	-21.74	-2.71-2.64	-25.82-2.86
1d	-17.07	-0.93-2.05	-22.10-2.60	$1d_{5/2}$	-17.24	-3.26-1.98	-23.84-2.48
				$1d_{3/2}$	-16.82	-	-19.96-2.79
2s	-15.44	-	-21.60-2.48	$2s_{1/2}$	-15.44	-	-21.60-2.48
1f	-11.64	-	-17.28-2.33	$1f_{7/2}$	-11.98	-	-20.78-2.16
				$1f_{5/2}$	-11.22	-	-13.54-2.57
2p	-9.34	-	-16.60-2.09	$2p_{3/2}$	-9.48	-	-17.59-2.09
				$2p_{1/2}$	-9.18	-	-14.62-2.12
1g	-5.69	-	-12.31-1.98	$1g_{9/2}$	-6.25	-	-17.75-1.89
				$1g_{7/2}$	-5.07	-	-6.58-2.11
2d	-3.16	-	-11.87-1.62	$2d_{5/2}$	-3.63	-	-13.60-1.78
				$2d_{3/2}$	-3.04	-	-9.15-1.33
3s	-2.77	-	-11.86-1.51	$3s_{1/2}$	-2.77	-	-11.86-1.51
1h	-0.30	-	-7.38-1.53	$1h_{11/2}$	-0.21	-	-14.52-1.66
				$1h_{9/2}$	-	-	-1.04-0.71
2f	-	-	-7.59-1.20	$2f_{7/2}$	-	-	-9.50-1.51
				$2f_{5/2}$	-	-	-5.24-0.73
2g	-	-	-3.60-0.99	$2g_{9/2}$	-	-	-5.50-1.22
				$2g_{7/2}$	-	-	-1.85-0.76
1i	-	-	-2.64-1.06	-	-	-	-

**Table 5 Root-mean-square distance of heavy hypernuclei  ${}^{208}_{\Lambda}Pb$  and  ${}^{208}_{\Sigma^{-}}Hg$  for different  $lj$  states**

Single-particle States	${}^{208}_{\Lambda}Pb$	${}^{208}_{\Sigma^{-}}Hg$		Single particle states	${}^{208}_{\Lambda}Pb$	${}^{208}_{\Sigma^{-}}Hg$	
	RMS distance (fm)	RMS distance (fm) (without Coulomb potential)	RMS distance (fm) (with Coulomb potential)		RMS distance (fm)	RMS distance (fm) (without Coulomb potential)	RMS distance (fm) (with Coulomb potential)
1s	3.59	4.15	3.37	$1s_{1/2}$	3.59	4.15	3.37
1p	4.25	5.05	4.21	$1p_{3/2}$	4.26	5.25	4.35
				$1p_{1/2}$	4.23	4.66	3.97
1d	4.73	5.99	4.86	$1d_{5/2}$	4.76	6.02	5.14
				$1d_{3/2}$	4.70	-	4.48
2s	4.39	-	4.76	$2s_{1/2}$	4.39	-	4.76
1f	5.13	-	5.44	$1f_{7/2}$	5.17	-	5.72
				$1f_{5/2}$	5.10	-	4.98
2p	4.88	-	5.47	$2p_{3/2}$	4.94	-	5.44
				$2p_{1/2}$	4.93	-	5.47
1g	5.50	-	6.02	$1g_{9/2}$	5.56	-	6.13
				$1g_{7/2}$	5.45	-	5.87
2d	5.45	-	6.31	$2d_{5/2}$	5.74	-	6.01
				$2d_{3/2}$	5.78	-	6.86
3s	6.13	-	6.45	$3s_{1/2}$	6.13	-	6.45
1h	48.53	-	6.67	$1h_{11/2}$	6.03	-	6.43
				$1h_{9/2}$	49.50	-	8.23
2f	-	-	7.14	$2f_{7/2}$	-	-	6.62
				$2f_{5/2}$	-	-	8.00
2g	-	-	7.77	$2g_{9/2}$	-	-	7.29
				$2g_{7/2}$	-	-	8.34
1i	-	-	7.39		-	-	-

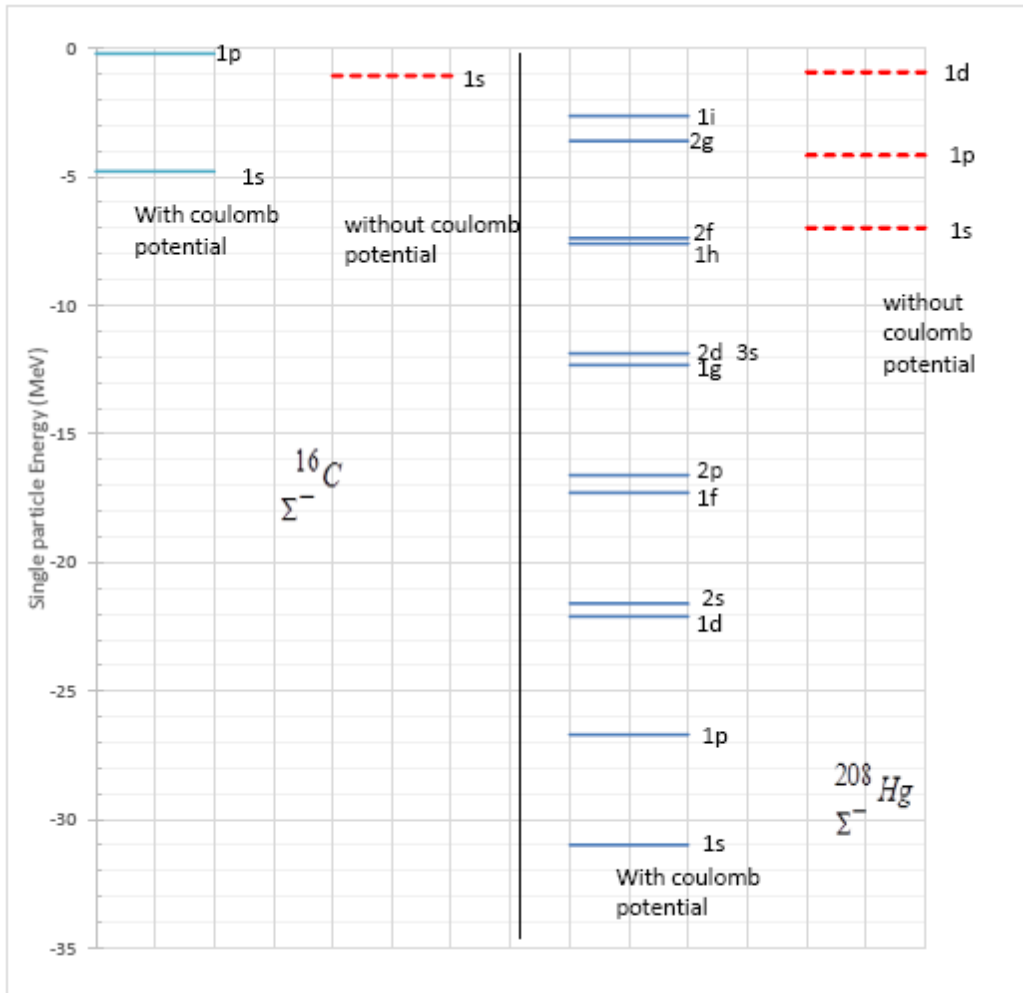


**Figure 1**  $\Sigma^-$  single particle states in  $^{16}_{\Sigma^-}C$  and  $^{208}_{\Sigma^-}Hg$  for different orbital angular momenta states with Coulomb and without Coulomb potential

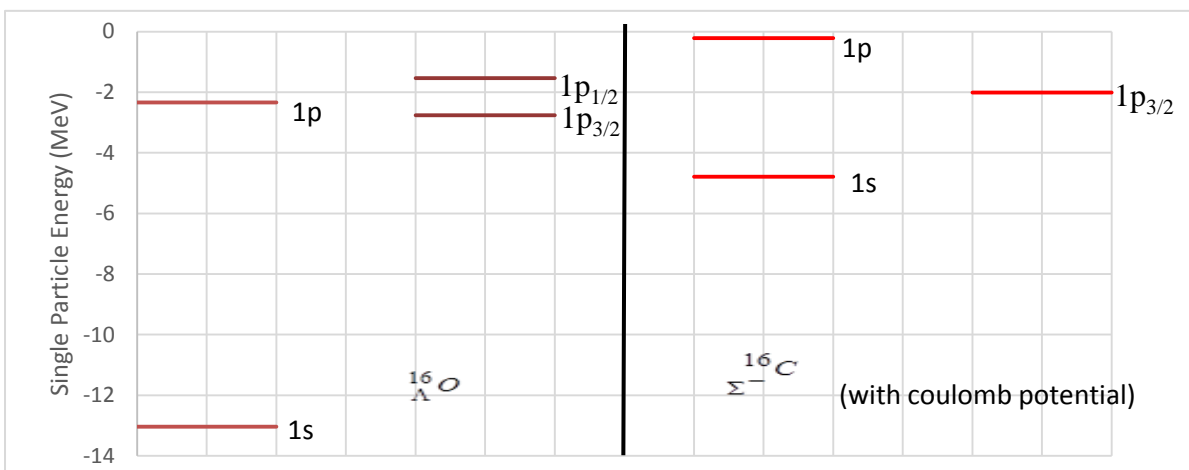


**Figure 2**  $\Lambda$  and  $\Sigma^-$  single particle states in light hypernuclei  $^{16}_{\Lambda}O$  and  $^{16}_{\Sigma^-}C$  for different  $l/j$  states

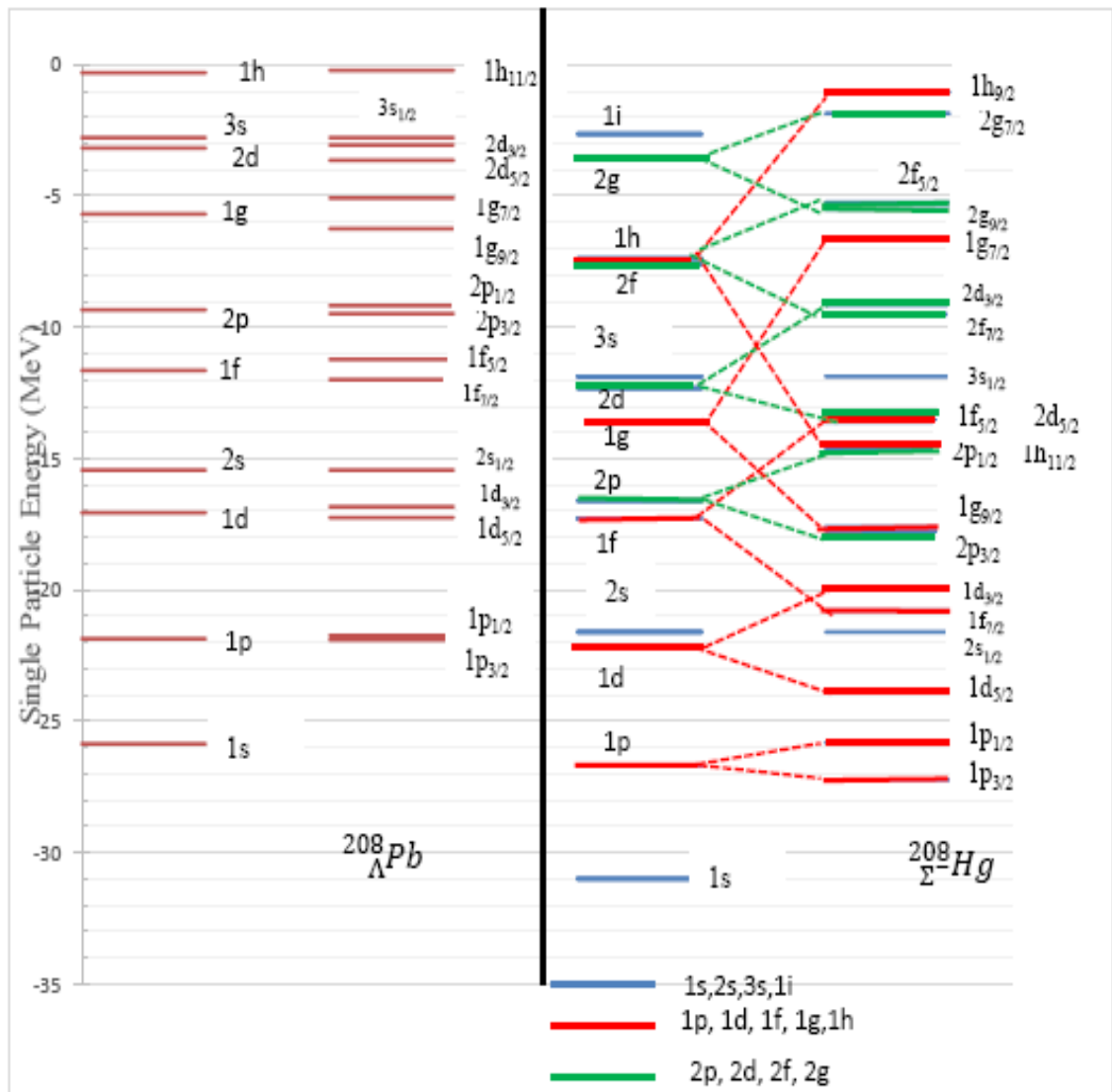


**Figure 3**  $\Lambda$  and  $\Sigma^-$  single particle states in heavy hypernuclei  $^{208}_{\Lambda}Pb$  and  $^{208}_{\Sigma^-}Hg$  for different  $lj$  states

The Coulomb interaction effect can be seen in figure (1). It is found that the energy states without Coulomb potentials are higher than that of with Coulomb potential in both light and heavy  $\Sigma^-$ -hypernuclei. Therefore, it can be concluded that it is important to take into account the attractive Coulomb potential between  $\Sigma^-$  and core nucleus for the calculation of single particle states in  $\Sigma^-$ -hypernuclei.

The energy eigen values and root-mean-square (RMS) distance of light hypernuclei  $^{16}_{\Lambda}O$  and  $^{16}_{\Sigma^-}C$  are presented table (2) and (3). And,  $\Lambda$  and  $\Sigma^-$  single particle states of those two light hypernuclei are displayed in figure (2). According to the calculated results, it is observed that the lowest binding state of  $^{16}_{\Lambda}O$  is  $1p_{1/2}$  state while  $1p_{3/2}$  state is lowest binding state in  $^{16}_{\Sigma^-}C$ . Moreover, it is found that single particle states of  $^{16}_{\Lambda}O$  are lower than that of  $^{16}_{\Sigma^-}C$  although

Coulomb potential is included in the calculation of energy states of  ${}_{\Sigma^-}^{16}\text{C}$  hyper nuclei. Therefore, it can be concluded that binding energy of light  $\Lambda$ -hypernucleus  ${}_{\Lambda}^{16}\text{O}$  is larger than that of light  $\Sigma^-$ -hypernucleus  ${}_{\Sigma^-}^{16}\text{C}$ .

Another observation is that the higher the single particle states, the larger the RMS distance with the increase in orbital angular momentum number in those two light hypernuclei.

The energy eigen values and RMS distance of heavy hypernuclei  ${}_{\Lambda}^{208}\text{Pb}$  and  ${}_{\Sigma^-}^{208}\text{Hg}$  are presented in table (4) and (5).  $\Lambda$  and  $\Sigma^-$  single particle states in those two heavy hypernuclei for different  $lj$  states are displayed in figure (3). According to the calculated results, it is found that the lowest binding state of  ${}_{\Lambda}^{208}\text{Pb}$  is  $1h_{11/2}$  state while  $1h_{9/2}$  state is lowest binding state in  ${}_{\Sigma^-}^{208}\text{Hg}$  when the Coulomb potential is included in the calculation of energy levels of  ${}_{\Sigma^-}^{208}\text{Hg}$  hypernucleus. In the heavy hypernuclei, binding energies of  ${}_{\Sigma^-}^{208}\text{Hg}$  is larger than that of  ${}_{\Lambda}^{208}\text{Pb}$  in different orbital angular momentum states.

It is found that RMS distance for  $\Sigma$  hyperon in  ${}_{\Sigma^-}^{208}\text{Hg}$  gradually increased with the decreasing of energy eigen values within the frame work of the Woods-Saxon central potential including with and without Coulomb potential.

It is also observed that energy splitting of  ${}_{\Sigma^-}^{208}\text{Hg}$  is larger than that of  ${}_{\Lambda}^{208}\text{Pb}$  with the increase in orbital angular momentum number. It is due to the larger spin-orbit potential strength of  $\Sigma$ -hypernuclei than that of  $\Lambda$ -hypernuclei.

The interesting result what we found in our calculation is that the RMS distance for  $\Sigma$ -hyperon in  ${}_{\Sigma^-}^{208}\text{Hg}$  gradually increased with the increasing of energy eigen values when the spin-orbit interaction is switched on.

In order to understand this strange behavior clearly, the potential and the corresponding wave function have been plotted for various  $lj$  states of  ${}_{\Sigma^-}^{208}\text{Hg}$  which are displayed in figure 4 (a) to (d). It is found that the attractive interaction strength of total spin  $j = l + s$  state is stronger than that of  $j = l - s$  state. The stronger interaction strength gives the greater binding energy. Moreover, the spin-orbit attractive potential works near the nuclear surface. Furthermore, the single-nucleon wave functions for  $j = l + s$  are more shifted to the outer region than that having spin state  $j = l - s$  and that is why the root-mean-square distance of nuclei for each spin state is larger although the binding energy is large. These effects could explain why both the rms value and binding energy are large.

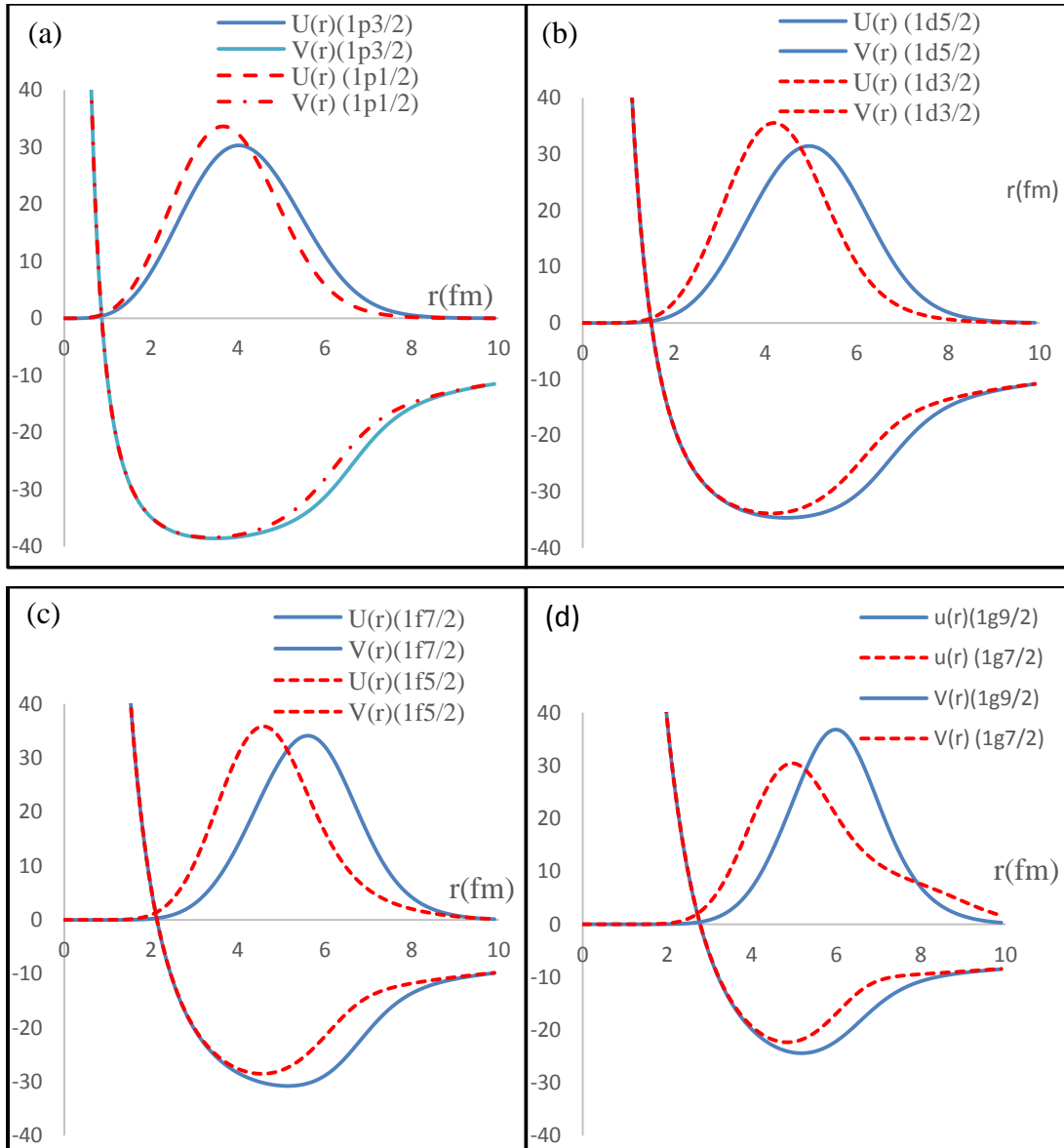


**Figure 4**  $\Sigma^-$  single-particle wave functions and potentials in  $^{208}\text{Hg}$  for  $\Sigma^-$

(a) 1p state and (b) 1d state(c) 1f state (d) 1g state

### Conclusion

We have investigated the characteristic of  $\Lambda$  and  $\Sigma$  hyperons in light hypernuclei  $^{16}_{\Lambda}O$  and  $^{16}_{\Sigma^-}C$  and heavy hypernuclei  $^{208}_{\Lambda}Pb$  and  $^{208}_{\Sigma^-}Hg$ . Single particle energy states and RMS distance of  $\Lambda$  and  $\Sigma$  hyperons are calculated by solving one body Schrödinger radial equation using power inverse iteration method numerically. For  $\Sigma$ -hypernuclei, Coulomb interaction is included beside Woods-Saxon central potential and Woods-Saxon spin-orbit potential in the calculation of energy eigen values to investigate the effect of Coulomb interaction. It is found that Coulomb interaction is important to take into account in the calculation of energy eigen values for  $\Sigma$  hypernuclei. And,

it is observed that the binding energy of light hypernucleus  ${}_{\Lambda}^{16}O$  is larger than that of  ${}_{\Sigma^{-}}^{16}C$ . But, binding energy of heavy hypernucleus  ${}_{\Lambda}^{208}Pb$  is smaller than that of  ${}_{\Sigma^{-}}^{208}Hg$  due to the Coulomb attractive interaction in heavy hypernucleus  ${}_{\Sigma^{-}}^{208}Hg$ . Therefore, it can be concluded that the  $\Sigma$ -single particle states are coulomb assistant nuclear states. It is found that the energy splitting of  $\Sigma$  hypernuclei is larger than that of  $\Lambda$  hypernuclei due to the large spin-orbit strength of  $\Sigma$  hypernuclei.

And, it is also found out the interesting observation that the root-mean-square distance of nuclei for each spin state of heavy  $\Sigma^{-}$ -hypernucleus is larger although the binding energy is large. Because, the spin-orbit attractive potential works near the nuclear surface and the single-hyperon wave functions for  $j = l + s$  are more shifted to the outer region than that having spin state  $j = l - s$ .

### Acknowledgements

I am deeply grateful to Dr Khin Swe Myint, Emeritus Professor, Rector (Rtd.), University of Mandalay, for her invaluable advices and discussion for this work. And, I thank to the member of Theoretical Nuclear Physics group of Physics department, University of Mandalay for their useful discussions.

### References

- Bando H, (1981), Prog. Theor. Phys. **66** 1349.  
 Bando H, Motoba T and Zofka J, (1990), Intl. J. Mod. Phys. **A 5** 4079 and references are therein.  
 Bertini R *et al.*, (1985), Phys. Lett. **158B** 19.  
 Bressani T *et al.*, (1989), NuovoCimento **A102** 491.  
 Dover C B, (1986), Proc. Int. Nucl. Phys. Conf. 99.  
 Hayano R S *et al.*, (1988), INS-Rep. **705**.  
 Harada T and Akaishi Y, (1990), *phys. Lett.* **B234** 455.  
 Pirner H J, (1979), Phys. Lett. **85B** 190.  
 Pirner H J and Povh B, (1982), Phys. Lett. **114B** 308.  
 Yamazaki T *et al.*, (1986), Nucl. Phys. **450** 1c.  
 Wünsch R and Zofka J, (1988), J. Phys. **B38** 755.